EPJ E
Soft Matter
www.epj.org

Eur. Phys. J. E **27**, 3–11 (2008) DOI: 10.1140/epje/i2008-10345-0

Physical aging of glassy PMMA/toluene films: Influence of drying/swelling history

F. Doumenc, H. Bodiguel and B. Guerrier

EDP SCIENCES Società Italiana Di Fisica Springer

Eur. Phys. J. E **27**, 3–11 (2008)
DOI 10.1140/epje/i2008-10345-0

THE EUROPEAN PHYSICAL JOURNAL E

Physical aging of glassy PMMA/toluene films: Influence of drying/swelling history

F. Doumenc[a], H. Bodiguel[b], and B. Guerrier[c]

Université Pierre et Marie Curie-Paris 6, Université Paris-Sud, CNRS, Laboratoire FAST, F-91405, France and Laboratoire FAST, Bat 502, Campus Universitaire, Orsay, F-91405, France

Received 8 February 2008
Published online: 25 July 2008 –

Abstract. Gravimetry experiments in a well-controlled environment have been performed to investigate aging for a glassy PMMA/toluene film. The temperature is constant and the control parameter is the solvent vapor pressure above the film (*i.e.* the activity). Several experimental protocols have been used, starting from a high activity where the film is swollen and rubbery and then aging the film at different activities below the glass transition. Desorption and resorption curves have been compared for the different protocols, in particular in terms of the softening time, *i.e.* the time needed by the sample to recover an equilibrium state at high activity. Non-trivial behaviors have been observed, especially at small activities (deep quench). A model is proposed, extending the Leibler-Sekimoto approach to take into account the structural relaxation in the glassy state, using the Tool formalism. This model well captures some of the observed phenomena, but fails in describing the specific kinetics observed when aging is followed by a short but deep quench.

PACS. 64.70.pj Polymers – 82.35.Lr Physical properties of polymers – 61.41.+e Polymers, elastomers, and plastics

1 Introduction

Numerous studies have recently been devoted to physical aging in glassy materials, but the observed phenomena due to non-equilibrium glassy dynamics are far from being really understood. Physical aging results in a slow evolution of the system physical properties with time, that depends on the whole sample history below the glass transition. Models and experiments concern a wide range of glassy materials, like spin glasses, colloidal suspensions, molecular glass, polymers, ... Non-trivial effects such as memory and rejuvenation have been observed in different systems when performing elaborate protocols like cycles or successive quenches [1–9]. To go deeper in the understanding of the glassy state, an important point is the characterization of the similarities as well as the specific features of the observed behaviors depending on i) the system under study, ii) the external control parameter used in aging experiments (temperature, mechanical treatment, solvent activity, . . .) and iii) the observed variables (measurements). The aim of this paper is to give new experimental results of complex aging phenomena for a polymer solution, when the control parameter is the solvent vapor pressure above the film (*i.e.* the activity) and the observation is the solvent concentration. We have used a polymethylmethacrylate (PMMA)/toluene solution at a given temperature $T_{\rm exp}$ (298 K) smaller than the glass transition temperature of the pure polymer, $T_{\rm gp}$ (395 K). Then the film is rubbery when the solvent concentration is high (swollen film) and glassy below a given solvent concentration. By changing the solvent vapor pressure above the film, it is possible to swell or dry the film and to study the glass transition induced by solvent desorption.

Due to its extensive use in coating and membrane technology, polymer film drying has been widely investigated. However, while many aging experiments reported in the literature are performed by changing the sample temperature, fewer works concern the effects of physical aging when the glass transition is induced by solvent sorption. Depending on the experimental set up, different variables have been observed and various theoretical approaches have been used to analyze the data. For example, Punsalan and Koros have studied the change in solubility due to aging for polymer membranes in CO_2 sorption experiments [10]. They have performed both dilation and sorption experiments and have explained the less sorptive capacity coupled to a larger swelling of the aged samples in the framework of the dual mode model.

[a] e-mail: doumenc@fast.u-psud.fr
[b] e-mail: Hugues.BODIGUEL-EXTERIEUR@eu.rhodia.com
[c] e-mail: guerrier@fast.u-psud.fr

McKenna and coworkers have performed several experiments, analysing the mechanical behavior (creep compliance) or volume change in polymer films when submitted to various aging cycles [11–13]. Time-P_{CO_2} superposition or Tool-Narayanaswamy-Moynihan(TNM)/Kovacs-Aklonis-Hutchinson-Ramos(KAHR) models are used to analyse the experimental data. The authors conclude that their results show a similar behavior for the temperature- and activity-induced glass transition qualitatively, while quantitative agreement is not always fulfilled. In the present study gravimetry experiments have been performed in a well-controlled environment experiments to study toluene sorption or desorption in PMMA films. The control parameter is the solvent vapor pressure above the film and the observed variable is the solvent content in the film. Various aging cycles have been tested in order to investigate complex aging histories, for example using the protocols performed by Bellon and coauthors [2,3] to highlight memory effects in temperature-induced glass transition. As already pointed out in a preliminary study [14], we obtain non-trivial behaviors when the solvent vapor pressure is decreased to zero during the cycle (deep quench). A model is proposed, extending the Leibler-Sekimoto approach [15] to time-dependent behaviors using the Tool formalism [16]. As will be seen, this model well captures some of the observed phenomena, but fails in describing the specific kinetics observed when aging is followed by a short but deep quench.

2 Experimental section

The polymer used was PMMA (Sigma-Aldrich) and the solvent toluene. According to the suppliers, PMMA glass transition temperature is $T_{\rm gp} = 395\,{\rm K}$, the molecular weight is 350000 g/mol and the polydispersity is between 4 and 5; toluene has a 99.9% purity. The densities of PMMA and toluene are $1170\,{\rm kg/m^3}$ and $867\,{\rm kg/m^3}$, respectively. Three samples have been used. The first one was obtained by slow drying of a PMMA/methylethylketone solution, transferred onto a $38\,\mu$m thick aluminium substrate (diameter 40 mm), and annealed at 373 K during a few days. Methylethylketone has a 99.7% purity (chromatography use). The two others were spin cast onto silicon wafers using a PMMA/toluene solution, transferred onto $38\,\mu$m thick aluminium substrates (diameters 40 mm and 42 mm), dried several days at ambient temperature and then dried 24 h in vacuum at 298 K. As the obtained results were found not sensitive to the sample preparation, no distinction between the three samples is made in the following. At the end of the experiments each sample was completely dried at 403 K and weighed, the aluminium substrate was cleaned in toluene to dissolve the PMMA film and weighed. Then the PMMA mass was deduced by difference. The PMMA mass for the three samples is about 0.9 mg so that the thickness of the polymer film evaluated from weighing is about $0.6\,\mu$m; its uniformity was checked using optical interferometry. Note that for such film thickness no influence of the thickness on glass transition is expected (*cf.*, for example, [17]).

The mass of the film in the presence of the solvent vapor was measured using a Hiden IGA balance which has the advantages of a good resolution ($\pm 1\,\mu$g) and long time stability (about $\pm 10\,\mu$g on one day, mainly due to the difference in solvent adsorption in the two parts of the beam). The measuring cell is filled with pure solvent vapor (no inert gas) whose temperature and pressure are accurately controlled: temperature is kept constant at $T = 298\,{\rm K} \pm 0.05$ and pressure P ranges from a few Pa (noted 0 Pa in the following) to 3.4×10^3 Pa with a stability ± 2 Pa. When estimating the solvent mass fraction from the balance data, the largest error comes from the uncertainty on the polymer mass ($+/-0.1$ mg), which leads to a large uncertainty (about 0.06) on the absolute value of the solvent mass fraction $\omega_{\rm s}$ at low solvent content (*i.e.* for small pressure). However even if the absolute value of $\omega_{\rm s}$ is poorly evaluated, the shape and slope of $\omega_{\rm s}$ *versus* P is not very affected.

As already mentioned in the introduction, one specific feature of the glassy state is the strong influence of the sample history on its dynamical properties. Then it is informative to perform various protocols to investigate aging behavior. Here the temperature is constant (298 K for all the experiments, that is 97 K below the glass transition temperature of dry PMMA) and the control parameter is the solvent vapor pressure above the film. Different kinds of solvent vapor pressure cycles have been used. Assuming that the solvent vapor behaves as an ideal gas, the activity of the solvent is given by $a = P/P_{\rm vs_0}$ (where $P_{\rm vs_0} = 3.79 \times 10^3$ Pa is the saturated vapor pressure of toluene at 298 K). In the following we use the activity as the control parameter to analyze the results. Before each run the pressure is maintained at or above $a = 0.9$ ($P > 3.4 \times 10^3$ Pa) during 160 min. The polymer film is then largely swollen, it contains about 50% of solvent which is well above the solvent concentration at the glass transition. A rough estimation of the glass transition temperature of a solution with 50% of solvent, using for example the Chow model (*cf.* the modelling section), gives $T \simeq 245\,{\rm K}$, that is more than 50 K below the temperature of the experiments. We can then assume that the film is molten, that the previous pressure history is erased and that the initial state of each run is well defined (*cf.* some comments on that point at the end of this section). A first family of pressure cycles consists in decreasing the pressure down to a given activity $a_{\rm min}$, where $a_{\rm min} = P_{\rm min}/P_{\rm vs_0}$, keeping $a = a_{\rm min}$ during a waiting time $t_{\rm min}$ and then increasing the activity again up to 0.9. These cycles are called $\mathcal{C}$ $(a_{\rm min}, t_{\rm min})$. More complex protocols have also been performed including a second stop at a constant activity $a_{\rm stop}$ during $t_{\rm stop}$. They are called $\mathcal{C}_{\rm D}$ cycle if the stop is made during the decreasing ramp and $\mathcal{C}_{\rm I}$ cycle if the stop is made during the increasing ramp. Examples of the three protocols are given in Figure 1. Unless explicitly mentioned, the ramp rate is 25 Pa/min in all the performed cycles. This rate of pressure variation comes from a compromise between the duration of the experiment (a $\mathcal{C}$ cycle takes about 5 hours when $a_{\rm min} = 0$ and $t_{\rm min}$ is small) and the diffusion time inside the film. The characteristic time of a decreasing ramp being about

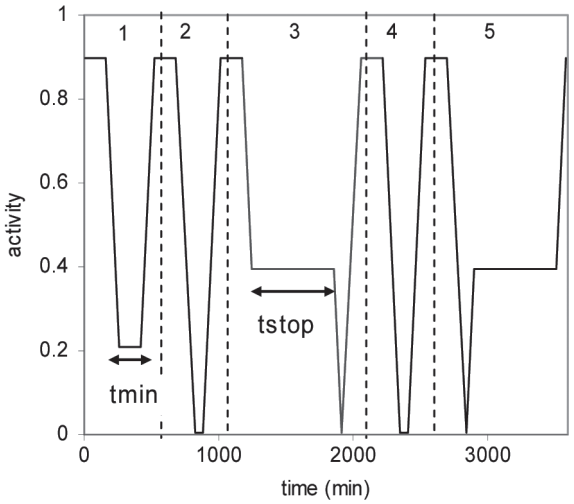

Fig. 1. Example of five successive cycles: cycles 1, 2 and 4 are $\mathcal{C}$ cycles with only one stop at $a_{\min} = 0.21$ during $t_{\min} = 160\,\text{min}$ for cycle 1 and at $a_{\min} = 0$ during $t_{\min} = 60\,\text{min}$ for cycles 2 and 4. Cycle 3 is a $\mathcal{C}_\text{D}$ cycle with a first stop at $a_{\text{stop}} = 0.4$ during $t_{\text{stop}} = 603\,\text{min}$, followed by a short stay at $a_{\min} = 0$ during $t_{\min} = 2\,\text{min}$. Cycle 5 is a $\mathcal{C}_\text{I}$ cycle with a short stay at $a_{\min} = 0$ during $t_{\min} = 1\,\text{min}$ followed by a stop at $a_{\text{stop}} = 0.4$ during $t_{\text{stop}} = 604\,\text{min}$.

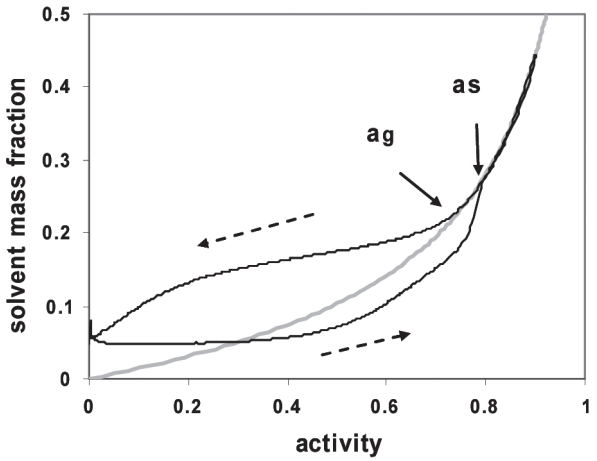

Fig. 2. Desorption/resorption isotherm: $\mathcal{C}(a_{\min} = 0,\ t_{\min} = 68\,\text{min})$ cycle (black line), Flory-Huggins model (grey line).

140 min and the film thickness 0.6 μm, the concentration gradient becomes non-negligible if the diffusion coefficient is smaller than $10^{-16}\,\text{m}^2/\text{s}$. That is less or of same order as the minimum value measured for PMMA/toluene at very small activities [18] and we assume in the following that the diffusion time is always shorter than the time variation of ω_s. At last a complete experiment (succession of many cycles) has been repeated on a blank sample (substrate without film) to make sure that the changes in solvent concentration induced by aging are greater than the possible drifts due to the balance itself.

Before comparing different aging protocols, some comments must be made on similar cycles performed at different times of the experiment (we call experiment the succession of many cycles of desorption/resorption on a same sample). The stop at high activity during about two hours before each cycle in the rubbery state was expected to lead to a similar initial state for each cycle. However, a small drift may be observed between similar cycles, *i.e.* the mass measured at a given activity and with the same pressure history slightly differs from one cycle to another. This drift is more important at the beginning of the experiment and decreases during about 15 cycles. Typically, the difference between two similar cycles decreases from about 15 μg between the first and ninth cycles (corresponding to a mass fraction difference less than 0.02) to about 1 μg between the seventeenth and twenty-fourth cycles (corresponding to a mass fraction difference less than 10^{-3}). This means that a very slow modification of the sample takes place during the experiment. Let us note that similar phenomena have already been pointed out by Laschitsch and co-authors in gravimetry experiments on thin polymer brushes [19], or by Bodiguel and Fretigny on mechanical experiments on thin polymer films [20]. Understanding this behavior should be an interesting point but is beyond the scope of this paper, especially as the amplitude of the drift is much smaller than the phenomena analysed in the following.

3 Qualitative description of a $\mathcal{C}$ cycle: equilibrium properties, glass transition and hysteresis

A typical example of solvent desorption and resorption during a $\mathcal{C}$ cycle ($a_{\min} = 0$, $t_{\min} = 68\,\text{min}$) is shown in Figure 2, where the solvent content is given in solvent mass fraction ω_s, directly deduced from mass measurements. Starting from a high activity where the film is swollen and rubbery (the solvent mass fraction is about 0.45), the first part of the desorption curve ($0.9 > a > a_\text{g}$) corresponds to the equilibrium isotherm of a rubbery polymer and can be described by a classical model such as the Flory-Huggins equation [21]

$$a = \varphi_\text{s} \times \exp[(1-\varphi_\text{s}) + \chi(1-\varphi_\text{s})^2], \qquad (1)$$

where φ_s is the solvent volume fraction and χ is the interaction parameter that characterises the polymer/solvent affinity and that slightly depends on the solvent volume fraction for PMMA/toluene.

Taking into account all uncertainties, the estimation of the glass transition activity a_g performed on various cycles leads to $a_\text{g} = 0.74 \pm 0.01$ which corresponds to a solvent vapour pressure at the glass transition $P_\text{g} = (2.8 \pm 0.05) \times 10^3\,\text{Pa}$. The interaction parameter χ is found equal to 0.4 ± 0.1, where the error bar takes account both of the dispersion of the results for the fit performed for various cycles and of the variation of χ in the range of φ_s involved. A good agreement with the previously published data is found in [22–25].

Below the activity a_g, the desorption curve moves away from the equilibrium isotherm: the film is glassy and an excess of solvent is observed as the relaxation times are

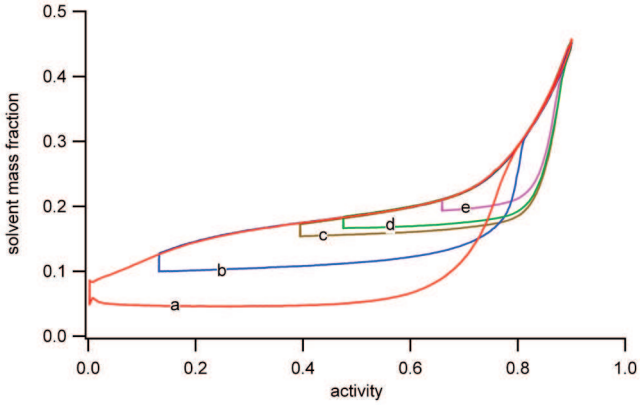

Fig. 3. (Colour on-line) Influence of aging activity $a_{\min}$: comparison of five experimental $\mathcal{C}(a_{\min}, t_{\min} \simeq 600\,\text{min})$ cycles; $a_{\min} = 0$ (red curve "a"), $a_{\min} = 0.13$ (blue curve "b"), $a_{\min} = 0.40$ (brown curve "c"), $a_{\min} = 0.47$ (green curve "d"), $a_{\min} = 0.66$ (magenta curve "e").

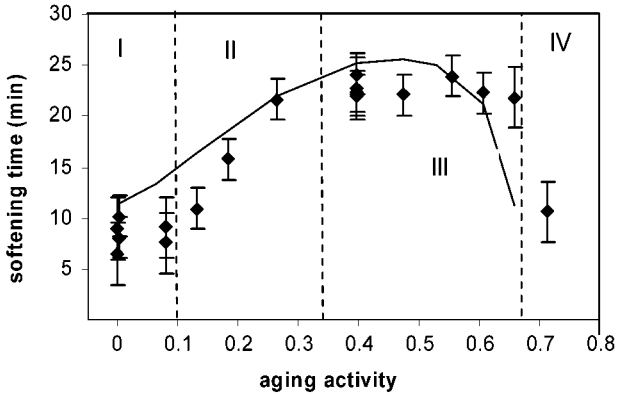

Fig. 4. Softening time as a function of the aging activity $a_{\min}$, for a waiting time $t_{\min} \simeq 600\,\text{min}$. Each black diamond corresponds to an experimental $\mathcal{C}(a_{\min}, t_{\min} \simeq 600\,\text{min})$ cycle. The continuous line has been obtained with the model presented in Section 4.2.

becoming too large for the material to follow the activity change. As can be seen in Figure 2, the solvent mass fraction does not decrease much between $a = 0.65$ and $a = 0.25$. Then the slope of the desorption curve increases when the activity becomes smaller than 0.2. When reversing the control parameter (increasing the activity from $a_{\min}$ up to 0.9), the resorption curve always shows a flat regime at the beginning, *i.e.* the solvent mass fraction remains almost constant. Then resorption occurs and the curve meets the equilibrium isotherm for an activity a_s greater than a_g (*cf.* Fig. 2). In the following the softening time θ is defined as the delay needed to meet the equilibrium isotherm again: $\theta = (a_s - a_g)/(\mathrm{d}a/\mathrm{d}t)$ where $\mathrm{d}a/\mathrm{d}t$ is constant in all the cycles presented here ($6.6 \times 10^{-3}\,\text{min}^{-1}$ for almost all the cycles). This softening time depends on the aging history below the glass transition, as thoroughly analysed in the following sections.

The downward curvature at low activity during decreasing ramps has previously been observed on different polymer/solvent systems and several models have been developed: the dual mode model is based on the existence of two types of sites for sorption, one in the dense polymer itself and the other in microvoids [26,27]; the mechanical model introduces an additional contribution in the chemical potential that accounts for the mechanical stresses induced by volume decrease under solvent loss, with the assumption that the glassy film is an elastic medium [15,28]. An extension of this last approach in order to take into account the structural relaxation in the glassy state will be presented in the following (*cf.* the modelling section).

4 Aging: results and discussion

4.1 Softening times for $\mathcal{C}$ cycles

Let us first compare $\mathcal{C}$ cycles with different $a_{\min}$ and the same large waiting time, $t_{\min}$ about 600 min. Five examples of desorption/sorption curves are given in Figure 3, and the results for all the experiments are gathered in Figure 4. As can be seen, the softening times are small for all the performed cycles (between 7 and 23 minutes). The aging/softening asymmetry, which is a well-known phenomenon in temperature-induced glass transition [29,30], is also observed here: the system softens in a few minutes only, while it has been aged for ten hours without reaching equilibrium. A non-trivial result is the non-monotonic behavior of the softening time as a function of the quench deepness. For $0.35 \leq a_{\min} \leq 0.65$, the softening time is about 23 min and does not depend on the aging activity (domain III in Fig. 4): all the resorption curves meet the equilibrium curve at about the same point, with $a_s \simeq 0.85$, as illustrated in Figure 3 for the three cycles c, d and e. But, when aging at very low activity (domain I), the softening time is much smaller (about 7 min); aging at intermediate activities leads to a transition regime between the two values (domain II). At last, aging at high activity ($a > 0.7$, domain IV) gives also a small softening time, because this activity is close to a_g (less deep quench). Moreover, when looking at the solvent loss during the aging at constant activity (Fig. 3), it can be seen that solvent desorption is at least as important at small activities, *i.e.* far from the glass transition, as for values much closer to a_g.

To go further in $\mathcal{C}$ cycles analysis, we have studied the influence of aging time for the two regimes, $a_{\min} < 0.1$ and $0.4 < a_{\min} < 0.65$ (*cf.* domains I and III in Fig. 4). For smaller waiting times the time spent during the decreasing and increasing ramps is no longer negligible and we introduce t_{tot} the total time elapsed by the film below the glass transition. The variations of the softening time θ as a function of t_{tot} are reported in Figure 5. For t_{tot} smaller than 1000 minutes, two distinct branches form: the upper one (blue to green full diamonds) corresponds to the domain III ($0.4 < a_{\min} < 0.65$ experiments). For the upper branch, as already observed in Figure 4, θ does not depend on the activity at which the film had elapsed time but only on t_{tot}. For the lower branch that corresponds to the domain I ($a_{\min} < 0.1$), whatever t_{tot} is (for $t_{\text{tot}} < 1000\,\text{min}$),

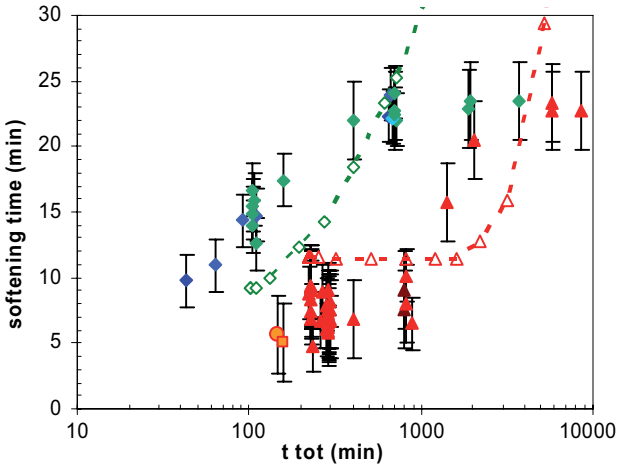

Fig. 5. (Colour on-line) Softening time as a function of the total time elapsed below the glass transition, $t_{\rm tot}$, for $\mathcal{C}(a_{\rm min}, t_{\rm min})$ cycles. Dark to light blue full diamonds correspond to $0.66 \leq a_{\rm min} \leq 0.47$ and green full diamonds to $a_{\rm min} = 0.40$ (Domain III in Fig. 4). Red full triangles correspond to $a_{\rm min} = 0$ (Domain I in Fig. 4). Orange full circle and square have also been obtained with $a_{\rm min} = 0$ but with different ramp rates (50 and 100 Pa/min). Empty green diamonds and red triangles have been obtained with the model, for the same cycles as the corresponding experimental full symbols.

θ is about constant and smaller than the value found in the upper branch. It is only for $t_{\rm tot}$ greater than 1000 minutes that the system becomes sensitive to the waiting time. At last, for very long waiting times, the points gather on a same asymptotic value that corresponds to a softening activity $a_{\rm s} = 0.89$. Above this activity the system softens whatever the history.

4.2 Model

To analyse these experimental results, a model has been developed, extending previous works performed for glassy polymers to our configuration. To express the solvent solubility in the glassy film, we have used a generalisation of the model proposed by Leibler and Sekimoto [15]. These authors have extended the Flory-Huggins model by introducing an additional term taking into account the stiffening of the system at the glass transition. We first recall the main points of their approach. The activity "a" is related to the osmotic pressure Π via the relation $RT\,{\rm Log}(a) = -\bar{v}_{\rm S}\Pi(\varphi_{\rm P}, T)$, where $\varphi_{\rm P}$ is the polymer volume fraction and where $\bar{v}_{\rm S}$, the solvent molar volume, is assumed constant. Besides, the bulk osmotic modulus $K(\varphi_{\rm P}, T)$ is defined as $K(\varphi_{\rm P}, T) = \varphi_{\rm P}\partial\Pi/\partial\varphi_{\rm P}$ (the bulk osmotic modulus can be measured by elastic deformation of the sample while allowing for the exchange of solvent between the sample and its surroundings).

Leibler and Sekimoto approximate the osmotic pressure by the sum of two contributions. The first one, $\Pi_{\rm rub}(\varphi_{\rm P}, T)$, corresponds to the osmotic pressure of the system in a rubbery state and is calculated from the classical Flory-Huggins theory for polymer solution in the rubbery state (*cf.* Eq. (1)). The second term corresponds to an additional contribution to the bulk osmotic modulus in the glassy state that accounts for the stiffening of the system at the glass transition. This additional contribution to the bulk modulus, $K_{\rm gl}$, only affects the domain $\varphi_{\rm P} \geq \varphi_{\rm Pg}$, where $\varphi_{\rm Pg}$ is the polymer volume fraction at the glass transition, that leads to the following expression [15]:

$$\Pi(\varphi_{\rm P}, T) = \int_0^{\varphi_{\rm P}} K(\varphi'_{\rm P}, T)\frac{{\rm d}\varphi'_{\rm P}}{\varphi'_{\rm P}} = \Pi_{\rm rub}(\varphi_{\rm P}, T) + \int_{\varphi_{\rm Pg}}^{\varphi_{\rm P}} K_{\rm gl}(\varphi'_{\rm P}, T)\frac{{\rm d}\varphi'_{\rm P}}{\varphi'_{\rm P}}. \quad (2)$$

Using this approximation of the osmotic pressure in the activity equation given previously yields to

$${\rm Log}(a) = {\rm Log}(1-\varphi_{\rm P}) + \varphi_{\rm P} + \chi\varphi_{\rm P}^2 - \frac{\bar{v}_{\rm S}}{RT}\int_{\varphi_{\rm Pg}}^{\varphi_{\rm P}} K_{\rm gl}\frac{{\rm d}\varphi'_{\rm P}}{\varphi'_{\rm P}}\,, \quad (3)$$

where R is the ideal-gas constant. As a further approximation, Leibler and Sekimoto assume that $K_{\rm gl}$ is constant and use the osmotic bulk modulus measured in the dry state to approximate $K_{\rm gl}$. As shown by these authors, this phenomenological elastic model well describes the deviation of the desorption isotherm from the equilibrium curve. But this model does not take into account viscoelastic stress relaxation in the glassy state at the time scale of the experiments, and then cannot reproduce aging effects. We propose an extension of the above model by introducing a time-dependent bulk modulus $K_{\rm gl}(t)$ which relaxes with the typical dynamics of the glassy polymer. Among the theoretical approaches used to analyse glassy dynamics, the Tool formalism and related models have been shown to successfully reproduce some complex aging behaviors in glassy polymers (*cf.* the review presented by Hodge and references herein [16]). These models assume that a glassy system relaxes towards equilibrium with a dynamics depending on its instantaneous structure, represented by a fictive temperature T^*. T^* would be the temperature of a system with this same structure but at equilibrium. We have extended this approach to our configuration, where the control parameter is the activity and the observed variable is the solvent concentration. Similarly to the fictive temperature in TNM formalism, we define a fictive polymer volume fraction $\varphi_{\rm P}^*(t)$ which would be the polymer volume fraction of the system at equilibrium, having the same structure. The dynamics is assumed to relax with a time distribution described by a stretched exponential, with exponent β. The mean relaxation time, $\langle\tau\rangle$ [31], depends on the system structure, *i.e.* on the fictive polymer volume fraction $\varphi_{\rm P}^*(t)$. The simplest way to introduce this dependence is to assume that the dynamics is mainly driven by the distance to the glass transition temperature. Then the characteristic time τ of the system is given by the Williams-Landel-Ferry (WLF) equation, where the temperature is simply shifted by a given quantity $\Delta T_{\rm g}(\varphi_{\rm P}^*) = (T_{\rm g}(\varphi_{\rm P}^*) - T_{\rm gp})$, that depends

on the fictive solvent content,

$$\tau(\varphi_{\rm P}^*) = \tau_0 \times \exp\left[\frac{B}{T - T_0 - \Delta T_{\rm g}(\varphi_{\rm P}^*)}\right], \qquad (4)$$

where T is the sample temperature (constant in our experiments) and where B, T_0 and τ_0 are constant for a given polymer. The absolute value of the shift $\Delta T_{\rm g}(\varphi_{\rm P}^*)$ increases with $\varphi_{\rm P}^*$, so that a system with a large fictive solvent content relaxes faster than a system close to equilibrium. For the constants τ_0 and B we have used the values given in [16] for PMMA, *i.e.* $\tau_0 = 8.29 \times 10^{-25}$ s, $B = 3430$ K. T_0 is set to 335.8 K. This value was slightly modified compared to the value reported in reference [16] in order to get a mean relaxation time of 100 s for $T = T_{\rm gp} = 395$ K, which corresponds to the glass transition of our dry PMMA sample. $\Delta T_{\rm g}(\varphi_{\rm P}^*)$ is deduced from the Chow model that gives the glass transition temperature of a solution as a function of the polymer volume fraction [32]:

$$\mathrm{Log}\left(\frac{T_{\rm g}^{\rm sol}}{T_{\rm gp}}\right) = \lambda[(1-\Theta^*)\times\mathrm{Log}(1-\Theta^*)+\Theta^*\,\mathrm{Log}\,\Theta^*], \quad (5)$$

where $\Theta^* = \Omega\frac{(1-\varphi_{\rm P}^*)}{\varphi_{\rm P}^*}$ and $\varphi_{\rm P}^*$ is the fictive polymer volume fraction. $T_{\rm gp}$ is the glass transition temperature of the dry polymer and $T_{\rm g}^{\rm sol}$ the one of the solution with polymer volume fraction $\varphi_{\rm P}^*$. λ and Ω are two parameters depending on the polymer and solvent properties [32] and are equal to 0.693 and 0.402, respectively, for our system.

At time t the system is then characterized by the real polymer volume fraction $\varphi_{\rm P}(t)$ and the fictive one $\varphi_{\rm P}^*(t)$, whose evolution as a function of $\varphi_{\rm P}(t)$ is given in the TNM approach by [16]

$$\varphi_{\rm P}^*(t) = \varphi_{\rm P}(0) + \int_0^t \frac{\partial\varphi_{\rm P}(t')}{\partial t'}\left\{1 - \exp\left[-\tilde{t}(t',t)^\beta\right]\right\}\mathrm{d}t', \qquad (6)$$

with $\tilde{t}(t',t) = \int_{t'}^t \frac{\mathrm{d}t''}{\tau[\varphi_{\rm P}^*(t'')]}$.

The initial condition at $t = 0$ corresponds to a point in the rubbery state (equilibrium state with $\varphi_{\rm P} \ll \varphi_{\rm Pg}$): then $\varphi_{\rm P}^*(t=0) = \varphi_{\rm P}(t=0)$ and the initial polymer volume fraction $\varphi_{\rm P}(t=0)$ is given by the Flory-Huggins model (Eq. (1)).

Extending the Leibler Sekimoto model (3), we assume that $K_{\rm gl}$ relaxes with the same dynamics as $\varphi_{\rm P}^*$. Then we get

$$\mathrm{Log}(a) = \mathrm{Log}(1-\varphi_{\rm P}) + \varphi_{\rm P} + \chi\varphi_{\rm P}^2 - \tilde{K}\int_0^t \frac{\exp\left[-\tilde{t}(t',t)^\beta\right]}{\varphi_{\rm P}(t')} \times \frac{\partial\varphi_{\rm P}(t')}{\partial t'}\mathrm{d}t', \qquad (7)$$

where it is assumed that the system is at equilibrium at $t = 0$ and where $\tilde{K} = \frac{\bar{v}_{\rm S} K_{\rm gl}}{RT}$. $K_{\rm gl}$ is about 10^9 Pa [15] and $\chi = 0.4$ (*cf.* experimental section).

The influence on the solubility of stresses induced by the solvent concentration variation in the glassy state is taken into account through this phenomenological model. Equation (7) gives the relation between the control parameter, *i.e.* the activity, and the measured quantity, the polymer volume fraction $\varphi_{\rm P}(t)$ in the sample. The resolution of equations (4) to (7), with the initial condition $\varphi_{\rm P}^*(t=0) = \varphi_{\rm P}(t=0)$, gives the evolution of $\varphi_{\rm P}$, $\varphi_{\rm P}^*$ and τ as a function of the activity evolution $a(t)$. Let us emphasize that the only adjustable parameter used to fit the data is β (the exponent of the stretched exponential), the other ones being issued from previous works or from polymer and solvent properties.

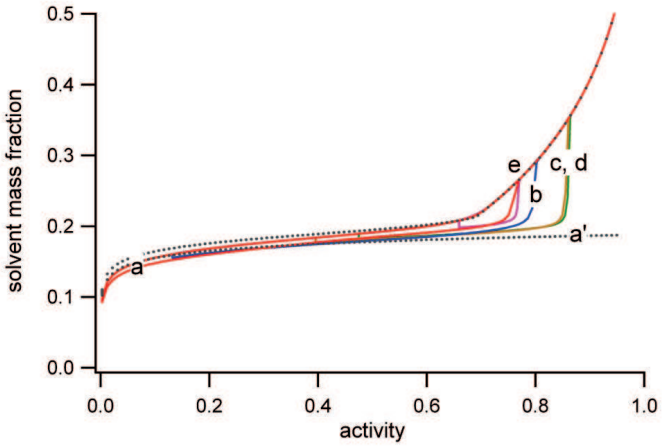

Fig. 6. (Colour on-line) Desorption and sorption isotherms obtained with the model presented in Section 4.2 for $\mathcal{C}(a_{\rm min}, t_{\rm min} \simeq 600\,\mathrm{min})$ cycles ($\beta = 0.3$). The colors and symbols are the same as in Figure 3. The dotted isotherm a′ was obtained with $\beta = 1$.

The above model was used to simulate experimental $\mathcal{C}$ cycles, and the parameter β was fitted on the data obtained with a waiting time of 600 min, that leads to $\beta = 0.3$, which is closed to the value $\beta = 0.34$ obtained in [16]. Comparing experimental and simulated isotherms (Figs. 3 and 6) shows that, on one hand, the decreasing ramp, the residual solvent content at $a = 0$ and the softening behaviour are quite well captured by the model for isotherms "a" to "d" corresponding to an aging at $a_{\rm min} = 0$ to $a_{\rm min} = 0.47$. The difference in the softening behaviour for experimental and simulated isotherms "e" (aging at $a = 0.66$) is due to a slight underestimation of the activity at the glass transition. Indeed, Chow and Flory-Huggins equations for $T = 298$ K gives $a_{\rm g} = 0.68$ while we get 0.74 from experiments. That is why the simulated "e" isotherm corresponds to an aging very close to the glass transition and then to a small softening time.

On the other hand, the model does not succeed in simulating the large hysteresis experimentally observed at the beginning of the increasing ramp. Numerical tests show that small changes in model parameters do not change the general trend of the simulated isotherms, except for β, the coefficient of the stretched exponential. Indeed, the model is very sensitive to the times distribution. To illustrate that point, simulation were also performed with $\beta = 1$, *i.e.* with a single exponential, keeping the same mean relaxation time. Figure 7 gives the evolution of the mean relaxation time during the cycles. As can be seen, even if very large relaxation times are reached at small activities

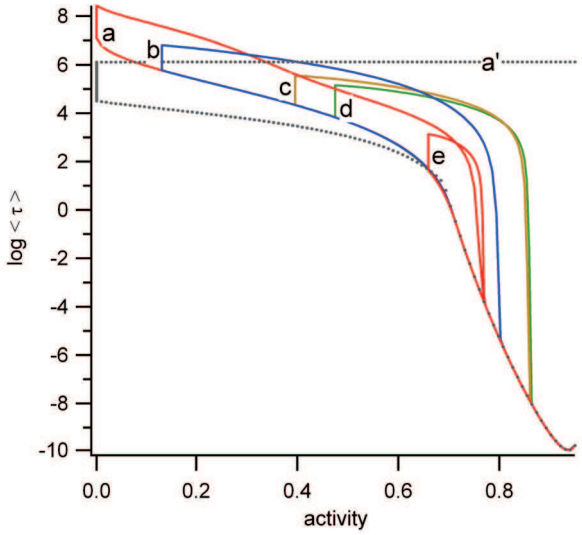

Fig. 7. (Colour on-line) Mean relaxation time during the $\mathcal{C}(a_{\min}, t_{\min} \simeq 600\,\text{min})$ cycles. The colors and symbols are the same as in Figure 6.

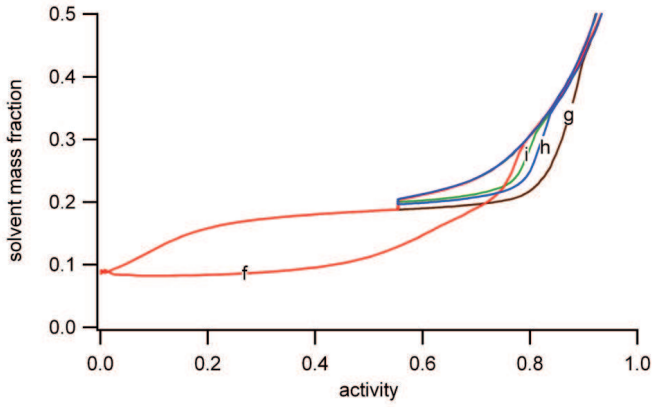

Fig. 8. (Colour on-line) Comparison of fours cycles with aging at $a = 0.55$. Green (i), blue (h) and brown (g) curves correspond to $\mathcal{C}$ cycles where the sample was aged at $a_{\min} = 0.55$ during $t_{\min} = 9\,\text{min}$ (green curve "i"), $t_{\min} = 54\,\text{min}$ (blue curve "h") and $t_{\min} = 610\,\text{min}$ (brown curve "g"). The red curve "f" is a $\mathcal{C}_\text{D}$ cycle, with a stop at $a = 0.55$ during 604 min followed by a short stay at $a = 0$ during 70 min.

with the stretched exponential distribution, the presence of small relaxation times in the distribution allows the system to soften again when the activity increases. On the contrary, in the case of the single exponential model, once large time constants are reached, the system cannot change anymore. This underlines the crucial role of the time distribution in the glassy state, as already pointed out by numerous experiments in polymer systems (see, for example, [33]). The dependence of the softening time with the activity and the non-monotony of the softening time is qualitatively well reproduced by the model, as shown in Figure 4 for $\mathcal{C}$ cycles with a waiting time of about 600 min: θ is small at low activity, increases for intermediate activity and decreases again close to the glass transition. As already said, the activity at the glass transition is underestimated, so that the boundary between the domains III and IV is shifted towards the small activities.

At least, if we compare the softening time as a function of t_{tot}, some of the experimental trends are also qualitatively captured by the model (empty symbols in Fig. 5): when aging at small activity, θ obtained by simulation is small (about 10 min) and constant unless very large waiting times are imposed to the sample ($t_{\text{tot}} > 2000\,\text{min}$). But the saturation experimentally observed for very long aging times is not obtained by the model; the softening time increases when the aging time increases, without reaching a plateau. As a conclusion, the model presented above allows to explain some of the main features of the aging behaviour for $\mathcal{C}$ cycles as the non-linear dependence of the softening time with the activity and underlines the importance of time distribution to explain the observed behaviours.

4.3 Softening times for $\mathcal{C}_\text{D}$ and $\mathcal{C}_\text{I}$ cycles

To go further in aging study and to highlight the specific behavior observed at small activities, coupling between aging at a given activity $(a_{\text{stop}}, t_{\text{stop}})$ and going through $a_{\min} = 0$ is studied by performing $\mathcal{C}_\text{D}$ and $\mathcal{C}_\text{I}$ cycles. In addition to the three steps of $\mathcal{C}$ cycles protocol (decreasing ramp, aging, increasing ramp), there is a run towards $a = 0$. It is performed after aging ($\mathcal{C}_\text{D}$ cycle) or before aging ($\mathcal{C}_\text{I}$ cycle) as illustrated by cycles 3 and 5 in Figure 1.

Let us first compare $\mathcal{C}$ and $\mathcal{C}_\text{D}$ cycles. An example is given in Figure 8 for four cycles corresponding to an aging at $a = 0.55$: three of them are $\mathcal{C}$ cycles with $t_{\min} = 9, 54$ and 610 min and the last one is a $\mathcal{C}_\text{D}$ cycle: after an aging at $a = 0.55$ for 604 min, the sample is brought to $a = 0$ for a short stay (70 min). This $\mathcal{C}_\text{D}$ cycle (red curve "f") is similar to the brown "g" $\mathcal{C}$ cycle of Figure 8, but adding a short stay at zero activity after aging. As can be seen, after the $\mathcal{C}_\text{D}$ cycle the system softens even faster than after an aging of only 9 minutes at $a_{\min} = 0.55$. This result was confirmed by other experiments and all the results obtained with an aging time $t_{\text{stop}} \simeq 600\,\text{min}$ at various activities and a short stay at $a = 0$ for a few minutes are gathered in Figure 9. Here again a short stay at $a_{\min} = 0$ is enough for the softening times to switch from the upper branch to the lower branch: the system "has forgotten" the ten hours stay at a_{stop}.

This behaviour is very different if we consider $\mathcal{C}_\text{I}$ cycles where the system ages ten hours at a_{stop} after a stay at zero. Indeed the softening behavior is then much closer to the corresponding $\mathcal{C}$ cycles, as shown by full green circles in Figure 9. These protocols ($\mathcal{C}_\text{D}$ and $\mathcal{C}_\text{I}$ cycles) have also been simulated with the TNM model described in the modelling section. Unlike for $\mathcal{C}$ cycles, the proposed model is not able to simulate the $\mathcal{C}_\text{D}$ aging specific behaviors. Indeed, simulated $\mathcal{C}_\text{D}$ cycles give softening times close to $\mathcal{C}$ or $\mathcal{C}_\text{I}$ cycles, as can be seen in Figure 9 where simulation results for the same cycles are also reported. As a last illustration, the three kinds of cycles are compared in Figure 10 for the same aging activity: $a_{\text{stop}} = 0.4$ and $t_{\text{stop}} = 600\,\text{min}$. The green "j" and blue "m" cycles

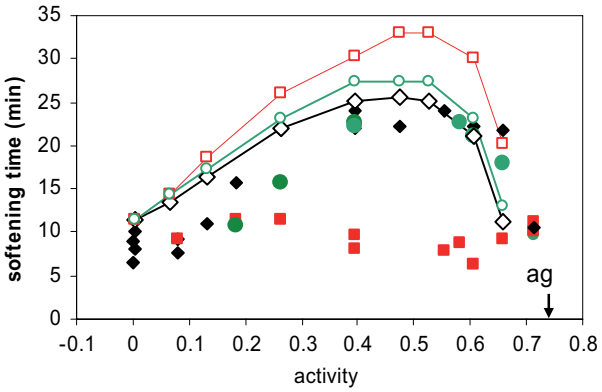

Fig. 9. (Colour on-line) Softening time as a function of the aging activity for a waiting time $\simeq 600$ min. Full black diamonds are experimental $\mathcal{C}$ cycles (error bars are not drawn anymore for clarity), full red squares are experimental $\mathcal{C}_{\rm D}$ cycles with a stay at $a = 0$ during less than 70 min after aging, full green circles are experimental $\mathcal{C}_{\rm I}$ cycles with a stay at $a = 0$ during less than 70 min before aging. Open symbols have been obtained with the TNM model for the same aging protocols (*i.e.* open black, red and green symbols correspond respectively to $\mathcal{C}$, $\mathcal{C}_{\rm D}$ and $\mathcal{C}_{\rm I}$ cycles).

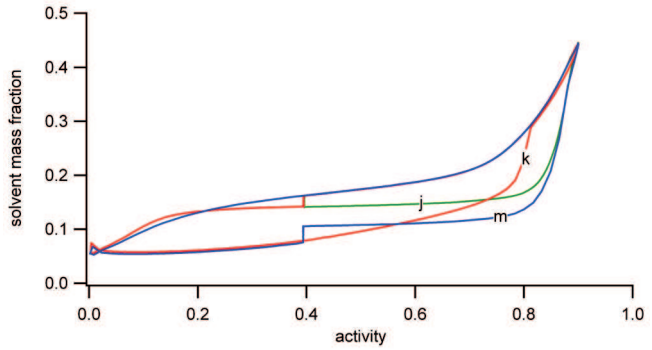

Fig. 10. (Colour on-line) Comparison of three cycles with aging at $a = 0.4$ during about 600 min. Green curve "j" $= \mathcal{C}$ cycle, red curve "k" $= \mathcal{C}_{\rm D}$ cycle with a short stay at $a = 0$ during 2 min after aging at $a = 0.4$, blue curve "m" $= \mathcal{C}_{\rm I}$ cycle with a short stay at $a = 0$ during 2 min before aging at $a = 0.4$.

($\mathcal{C}$ and $\mathcal{C}_{\rm I}$) soften together, with $a_{\rm s}$ about 0.9 ($\theta \simeq 23$ min) while the red "k" $\mathcal{C}_{\rm D}$ cycle meets the equilibrium much faster, with $a_{\rm s} = 0.8$ ($\theta \simeq 9$ min). A non-trivial coupling between the activity, solvent concentration, stress distribution, and film structure should be taken into account to capture these effects.

4.4 Critical discussion of the model

Although the model allows capturing some specific behaviour of aging in glassy films, it is necessary to enlarge it in order to take into account the phenomena observed at very low activities that are reported above, the large hysteresis between up and down pressure ramps and apparent rejuvenation that is observed whenever the system is brought to zero activity. This is beyond the scope of this paper and we only point out some simplifying assumptions that could be released in order to improve the solubility model on the one hand, and the dynamics description on the other hand. First the derivation of the solubility assumes constant molar volume for the solvent and the polymer. This assumption may have some influence especially at very small activities, where the solvent molar volume has been observed to decrease significantly [10]. Then in our model the dynamics is the same for structural relaxation (accounted by the fictive concentration) and stress relaxation, and is governed by a time distribution that depends on only one variable, the fictive concentration. A more complex description taking into account the coupling between volume, polymer concentration and stress may be a possible extension [36]. At least, the heterogeneities of the system are only taken into account through the width of the time distribution. Recent approaches that model the time evolution of the spatial heterogeneities of solvent, polymer and free-volume concentration [34,35] may improve the description of the dynamics. Heterogeneities of stress may also lead to non-trivial behavior, especially in the non-linear regime.

5 Conclusion

Several kinds of aging cycles have been performed on polymer/solvent films, by changing the solvent vapor pressure above the film and weighing the film during aging. Desorption and resorption curves have been compared for the different protocols, in particular in terms of the softening time, *i.e.* the time needed by the sample to recover an equilibrium state at high activity. Unexpected behaviors have been observed, especially at small activities. First experiments comparing cycles with a waiting time at a given activity followed by a resorption curve ($\mathcal{C}$ cycle) show that:
–at intermediate activities, the softening time is independent of the aging activity but depends on the aging time;
–at small activity the softening time is small and constant, except if the waiting time is very long (> 1000 min). An extension of the Leibler-Sekimoto model, using the Tool formalism, was developed for our experimental configuration: this model was shown to successfully reproduce some of these results, at least qualitatively.

More complex cycles, where aging is followed by a short stay at $a = 0$ ($\mathcal{C}_{\rm D}$ cycle), exhibit more complex behaviors that are not captured by the proposed model: indeed a short stay at small activity is enough to erase previous aging effects. Hopefully these experimental results will bring new insights on the problem of glassy state dynamics as they should be analysed in the light of recent glassy theoretical models. To go further in the understanding of solvent-induced glass transition, other kinds of experimental protocols as great activity steps before aging (instead of slow ramps) may be performed. Another very interesting development should be the simultaneous observation of both the film thickness and solvent content, in order to get information on the coupled evolution of the two

variables solvent content and excess volume and to compare the dynamics of film compaction and of solvent release [37].

The authors thank D. Long for helpful discussion. This work was partly supported by a "PPF contract" of the University Paris-Sud, France.

References

1. O. Araki, T. Shimamoto, T. Yamamoto, T. Masuda, Polymer **42**, 4433 (2001).
2. L. Bellon, S. Ciliberto, C. Laroche, Europhys. Lett. **51**, 551 (2000).
3. L. Bellon, S. Ciliberto, C. Laroche, Eur. Phys. J. B **25**, 223 (2002).
4. V. Dupuis, E. Vincent, J.P. Bouchaud, J. Hammann, A. Ito, H. Haruga Katori, Phys. Rev. B **64**, 174204 (2001).
5. J.M. Hutchinson, Prog. Polym. Sci. **20**, 703 (1995).
6. F. Krzakala, F. Ricci-Tersenghi, J. Phys. Conf. Ser. **40**, 42 (2006).
7. Y. Miyamoto, K. Fukao, H. Yamao, K. Sekimoto, Phys. Rev. Lett. **88**, 225504 (2002).
8. T. Narita, C. Beauvais, P. Hébraud, F. Lequeux, Eur. Phys. J. E **14**, 287 (2004).
9. H. Yardimci, R.L. Leheny, Europhys. Lett. **62**, 203 (2003).
10. D. Punsalan, W.J. Koros, Polymer **46**, 10214 (2005).
11. M. Alcoutlabi, F. Briatico-vangosa, G.B. McKenna, J. Polym. Sci. Part B **40**, 2050 (2002).
12. Y. Zheng, G.B. McKenna, Macromolecules **36**, 2387 (2003).
13. Y. Zheng, R.D. Priestley, G.B. McKenna, J. Polym. Sci. Part B **42**, 2107 (2004).
14. F. Doumenc, B. Guerrier, C. Allain, Europhys. Lett. **76**, 630 (2006).
15. L. Leibler, K. Sekimoto, Macromolecules **26**, 6937 (1993).
16. J.M. Hodge, J. Non-Cryst. Solids **169**, 211 (1994).
17. R. Priestley, M.K. Mundra, N.J. Barnett, L.J. Broadbelt, J.M. Torkelson, Austr. J. Chem. **60**, 765 (2007).
18. A.C. Dubreuil, F. Doumenc, B. Guerrier, C. Allain, Macromolecules **36**, 5157 (2003).
19. A. Laschitsch, C. Bouchard, J. Habicht, M. Schimmel, J. Ruhe, D. Johannsmann, Macromolecules **32**, 1244 (1999).
20. H. Bodiguel, C. Fretigny, Eur. Phys. J. E **19**, 185 (2006).
21. P.J. Flory, *Principles of Polymer Chemistry* (Cornell University Press, 1995).
22. A.C. Saby-Dubreuil, B. Guerrier, C. Allain, D. Johannsmann, Polymer **42**, 1383 (2001).
23. J. Brandrup, E.H. Immergut, *Polymer Handbook* (Wiley Interscience, New York, 1989).
24. A.F.M. Barton, *CRC Handbook of Polymer-Liquid Interaction Parameters and Solubility Parameters* (CRC Press, 1990).
25. C. Wohlfarth, *Vapor-Liquid Equilibrium Data of Binary Polymer Solutions* (Elsevier, Amsterdam, 1994).
26. V.T. Stannett, W.J. Koros, D.R. Paul, H.K. Lonsdale, R.W. Baker, Adv. Polym. Sci. **32**, 69 (1979).
27. A.R. Berens, Polym. Eng. Sci. **20**, 95 (1980).
28. G.G. Lipscomb, AIChE J. **36**, 1505 (1990).
29. A.J. Kovacs, J. Polym. Sci. **30**, 131 (1958).
30. S. Merabia, D. Long, J. Chem. Phys. **125**, 234901 (2006).
31. C.P. Lindsey, G.D. Patterson, J. Chem. Phys. **73**, 3348 (1980).
32. T.S. Chow, Macromolecules **13**, 362 (1980).
33. Bodiguel, F. Lequeux, H. Montes, J. Stat. Mech. P01020 (2008).
34. D. Long, F. Lequeux, Eur. Phys. J. E **4**, 371 (2001).
35. M. Souche, D. Long, Europhys. Lett. **77**, 48002 (2007).
36. S.L. Simon, J.-Y. Park, G.B. McKenna, Eur. Phys. J. E **8**, 209 (2002).
37. H. Richardson, M. Sferrazza, J.L. Keddie, Eur. Phys. J. E **12**, 437 (2003).